

Original scientific paper

## NONLINEAR VIBRATION RESPONSE OF PIEZOELECTRIC NANOSENSOR: INFLUENCES OF SURFACE/INTERFACE EFFECTS

Sayyid H. Hashemi Kachapi

Department of Mechanical Engineering, Babol Noshirvani University of Technology, Iran

**Abstract.** *In the present work, surface/interface energy effects for pull-in instability analysis on dimensionless natural frequency (DNF) and nonlinear dynamics response (NDR) of piezoelectric nanosensor (PENS) subjected to nonlinear electrostatic excitation and harmonic force are studied using Gurtin–Murdoch (GM) surface/interface energy approach. To achieve this purpose, the Hamilton’s approach, assumed mode and Lagrange–Euler’s theories and also arc-length continuation and complex averaging methods are used to investigate influences of surface/interface parameters of PENS such as Lamé’s constants, residual stress, piezoelectric constants and mass density for analysis of pull-in instability voltage.*

**Key words:** *Pull-in instability, Nonlinear dynamic response, Piezoelectric nanosensor, Surface/interface effects, Arc-length continuation, Nonlinear electrostatic excitation*

### 1. INTRODUCTION

Nanomechanical sensors and resonators especially for piezoelectric nanostructures, due to small size and mass and their unique properties, are widely used in advanced engineering applications and industry [1-3]. In the last decade, there has been a great deal of research into the vibrations and dynamics analysis especially the pull-in instability phenomenon of such nanostructures, some of which will be mentioned in the following. Farokhi et al. used FE approach to analyze nonlinear responses of static and dynamic and pull-in behavior for nano resonator with electrostatic excitation [4]. Prasanth et al. worked on pull-in behaviour of a micro resonator considering large elastic deflection [5]. Surface energy approach is utilized by Pourkiaee et al. to study nonlinear vibration of nano beam resonator with piezoelectric layer and electrostatic excitation [6]. Karimipour et al. presented nonclassical

---

Received June 12, 2021 / Accepted October 23, 2021

**Corresponding author:** Sayyid H. Hashemi Kachapi

Department of Mechanical Engineering, Babol Noshirvani University of Technology, P.O. Box 484, Shariati Street, Babol, Mazandaran47148-71167, Iran

E-mail: sha.hashemi.kachapi@gmail.com

theories to study pull-in behavior of thin plate activator [7]. In the work by Nikpourian et al., nonlinear dynamics analysis in micro beam resonator with piezoelectric layer and electrostatic force investigated using size dependent approach [8]. Investigation of pull-in phenomenon in NEMS and MEMS is studied by Zhang et al. [9]. Pull-in instability behavior of microbeams and Nano Bridge are presented by Sedighi et al. using strain gradient approach [10, 11]. Pull-in instability behavior of nanostructures such as nano bridges, NEMS and nanobeams, are presented by Tadi Beni et al. using non classical theories such as a modified version of coupled stress method [12-14]. Dynamic Pull-in and damage reconnaissance of micro structures is presented by Tajalli et al. [15]. Also the modified version of coupled stress method is utilized by Farokhi et al. to analyze resonant and pull-in behavior of carbon nanotube based resonators [16]. Stability analysis and nonlinear vibrations of structures such as plates and shells in theoretical and experimental cases are also presented by Amabili [17]. Bornassi et al. utilized nonlocal model to analyze pull-in phenomenon of NEMS [18]. For consideration of non-classical surface parameters of nanostructures, surface/interface energy approach is presented [19, 20]. Recently, using surface effect, buckling and postbuckling analysis and also vibration behavior of nano structures with piezoelectric layers are studied by Fang et al. [21, 22]. Also, Hashemi Kachapi et al. presented Gurtin–Murdoch surface/interface theory to investigate linear and nonlinear vibration analysis of piezoelectric nanostructures [23-28]. In the mentioned papers, the following effects have been studied: the effects of all surface/interface energy parameters; mechanical and structural properties of nanostructures and piezoelectric layers; van der Waals force; visco-Pasternak effects on the undamped and damped natural frequencies; parametric studies, such as the effects of different boundary conditions; different geometric ratios; structural parameters; electrostatic and harmonic excitation on the nonlinear frequency response and stability analysis. Fan utilized surface energy effects to enlarge the capability of piezoelectric/piezomagnetic energy harvester [29].

Despite a great number of researches on nanosensors dynamics and vibration, consideration of surface/interface energy effects on pull-in stability and vibration analysis of nanosensor with piezoelectric layers and electrostatic excitation have not been studied yet. In the present study, using arc-length continuation and complex averaging method [30], pull-in instability behavior of piezoelectric nanosensor are studied on dimensionless natural frequency and nonlinear dynamics response considering surface/interface energy effects.

## 2. MATHEMATICAL FORMULATION

A cylindrical piezoelectric nanosensor subjected to the combined electrostatic force and harmonic excitation is shown in Fig. 1.

Based on the surface/interface effect of Gurtin–Murdoch theory, the normal stresses  $\sigma_{xx}$  and  $\sigma_{\theta\theta}$  can be written as [19-26]

$$\sigma_{xx(N,p)} = C_{11(N,p)}\varepsilon_{xx} + C_{12(N,p)}\varepsilon_{\theta\theta} - e_{31p}\bar{E}_{xp} + \frac{v_{(N,p)}\sigma_{zz}}{1-v_{(N,p)}} \quad (1)$$

$$\sigma_{\theta\theta(N,p)} = C_{21(N,p)}\varepsilon_{xx} + C_{22(N,p)}\varepsilon_{\theta\theta} - e_{32p}\bar{E}_{\theta p} + \frac{v_{(N,p)}\sigma_{zz}}{1-v_{(N,p)}}, \quad (2)$$

$$\sigma_{x\theta(N,p)} = C_{66(N,p)}\gamma_{x\theta}, \quad (3)$$

where based on nonclassical continuum model,  $\sigma_{zz}$  is expressed as following

$$\sigma_{zz} = \frac{z}{h_N + h_p} \left( (\tau_0^S + \tau_0^I) \left( \frac{\partial^2 w}{\partial x^2} + \frac{1}{R^2} \frac{\partial^2 w}{\partial \theta^2} \right) - (\rho^S + \rho^I) \frac{\partial^2 w}{\partial t^2} \right), \quad (4)$$

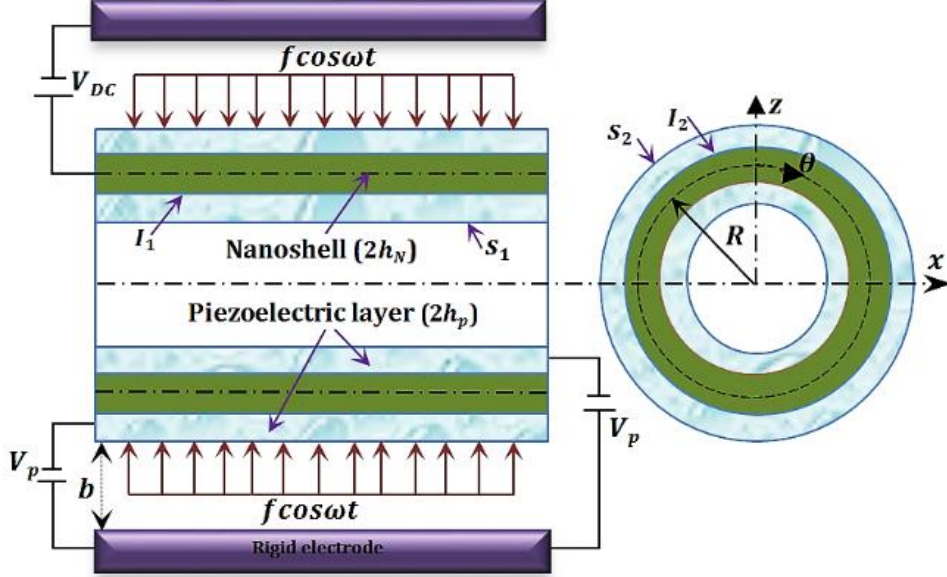


**Fig. 1** Piezo-harmonic-electrostatic nanosensor subjected to electrostatic harmonic excitation

Also all coefficients and phrases of Eqs. (1-4) such as displacement fields, nonlinear deflection and curvatures, relations of surface/interface theory and etc. can be observed in complete detail in reference [25].

By applying the assumed mode and Lagrange-Euler approaches, the governing equations and boundary conditions of PENS are obtained. For this purpose, the total strain energy of PENS considering the surface/interface effect can be presented as:

$$\pi = \frac{1}{2} \int_0^L \int_0^{2\pi} \left\{ N_{xx} \varepsilon_{xx}^0 + N_{\theta\theta} \varepsilon_{\theta\theta}^0 + N_{x\theta} \gamma_{x\theta}^0 + M_{xx} \kappa_{xx} \right. \\ \left. + M_{\theta\theta} \kappa_{\theta\theta} + M_{x\theta} \kappa_{x\theta} + \eta_{33} \bar{E}_{zp}^2 h_p \right\} R d\theta dx \quad (5)$$

In Eq. (5), the forces ( $N$ ) and moment ( $M$ ) resultants are determined in reference Hashemi Kachapi et al. [25]. The kinetic energy of the PENS can be written as:

$$T = \frac{1}{2} \iint \left\{ I \left( \left( \frac{\partial u}{\partial t} \right)^2 + \left( \frac{\partial v}{\partial t} \right)^2 + \left( \frac{\partial w}{\partial t} \right)^2 \right) \right\} R d\theta dx \quad (6)$$

where

$$I = \int_{-h_N}^{h_N} \rho_N dz + \int_{-h_N-h_p}^{-h_N} \rho_p dz + \int_{h_N}^{h_N+h_p} \rho_p dz + \rho^{S,I} = 2\rho_N h_N + 2\rho_p h_p + 2\rho^S + 2\rho^I$$

Also, the work done on the PENS due to the viscoelastic foundation, nonlinear electrostatic excitation and the harmonic force, respectively, can be presented as [25]

$$W_{vm} = - \int_0^L \int_0^{2\pi} \int_0^w \left( K_w w - K_p \nabla^2 w + C_w \frac{\partial w}{\partial t} \right) dw R d\theta dx, \quad (7)$$

$$W_e = \int_0^L \int_0^{2\pi} \int_0^w \frac{\pi \gamma V_D^2 c}{\sqrt{(b-w)(2R+b-w)} \left[ \cosh^{-1} \left( 1 + \frac{b-w}{R} \right) \right]^2} dw R d\theta dx \quad (8)$$

$$W_f = \int_0^L \int_0^{2\pi} \int_0^w (f \cos \omega t) dw R d\theta dx, \quad (9)$$

where all coefficients and phrases of Eqs. (7-9) can be seen in reference [25].

By applying of Hamilton's principle and substituting Eqs. (5-9) into Hamilton's principle and using dimensional parameters [25], the governing equations of motion and boundary conditions for PENS are obtained. In following using least-squares polynomial format of electrostatic force and by using the displacement and shear deformation in the assumed mode method and by applying non-dimensional strain and kinetic energies Eqs. (5) and (6) and also non-dimensional works Eqs. (7-9) and substituting in the Lagrange-Euler equations, the dimensionless equations of motion is obtained to the following equations:

$$[(M)_u^u]\{\ddot{u}\} + [(K)_u^u]\{\bar{u}\} + [(K)_u^v]\{\bar{v}\} + [(K)_u^w]\{\bar{w}\} + [(NL)_u^w]\{\bar{w}^2\} = \bar{F}_{up}, \quad (10)$$

$$[(M)_v^v]\{\ddot{v}\} + [(K)_v^u]\{\bar{u}\} + [(K)_v^v]\{\bar{v}\} + [(K)_v^w]\{\bar{w}\} + [(NL)_v^w]\{\bar{w}^2\} = \bar{F}_{vp}, \quad (11)$$

$$\begin{aligned} & [(M)_w^w]\{\ddot{w}\} + [(c)_w^w]\{\dot{w}\} + [(K)_w^u]\{\bar{u}\} + [(K)_w^v]\{\bar{v}\} + [(K)_w^w - \bar{F}_{e2}(K_e)_w^w]\{\bar{w}\} \\ & + [(NL)_w^u]\{\bar{w}\bar{u}\} + [(NL)_w^v]\{\bar{w}\bar{v}\} + [(NL)_w^w - \bar{F}_{e3}(NL_{2e})_w^w]\{\bar{w}^2\} \\ & + [(NL)_w^w - \bar{F}_{e4}(NL_{3e})_w^w]\{\bar{w}^3\} = \bar{F}_{we} + \bar{F}_{wp} + [\bar{F} \cos \bar{\Omega} \tau], \end{aligned} \quad (12)$$

where all the coefficients and phrases of Eqs. (10-12) are presented in reference [25].

In order to study the nonlinear dynamics response, arc-length continuation and complex averaging approaches are presented [25-26, 28].

Verification, comparison and convergence study is investigated in reference Hashemi Kachapi et al. with full details for PENS [25]. In this section, pull-in instability analysis on dimensionless natural frequency and nonlinear dynamics response are presented. For this purpose, different boundary condition such as clamped edge (CC), simply supported edge (SS), clamped-simply supported edge (CS) and, clamped-free edge (CF) are presented.

### 3. RESULTS AND DISCUSSIONS

The bulk and surface/interface material properties of Aluminum (Al) nanoshell and PZT piezoelectric layer are shown in Tables 1 and 2, respectively [24].

**Table 1** Bulk and surface/interface properties of Al

$E_N(\text{GPa})$	$\nu_N$	$\rho_N(\text{kg/m}^3)$	$\lambda^I(\text{N/m})$	$\mu^I(\text{N/m})$	$\tau_0^I(\text{N/m})$	$\rho^I(\text{kg/m}^2)$
70	0.33	2700	3.786	1.95	0.9108	$5.46 \times 10^{-7}$

**Table 2** Bulk and surface/interface properties of PZT-4

$C_{11p}(\text{GPa})$	$C_{22p}(\text{GPa})$	$C_{12p}(\text{GPa})$	$C_{21p}(\text{GPa})$	$C_{66p}(\text{GPa})$	$E_p(\text{GPa})$
139	139	77.8	77.8	30.5	95
$\nu_p$	$\rho_p(\text{kg m}^{-3})$	$\eta_{33p}(10^{-8} \text{ F})$	$\lambda^S(\text{N/m})$	$\mu^S(\text{N/m})$	$\tau_0^S(\text{N/m})$
0.3	7500	8.91	4.488	2.774	0.6048
$e_{31p}(\text{C/m}^2)$	$e_{32p}(\text{C/m}^2)$	$e_{31p}^S(\text{C/m})$	$e_{32p}^S(\text{C/m})$	$\rho^S(\text{kg/m}^2)$	
-5.2	-5.2	$-3 \times 10^{-8}$	$-3 \times 10^{-8}$	$5.61 \times 10^{-6}$	

The others geometrical and physical parameters of PENS are presented in Table 3 [24, 25].

**Table 3** The geometrical and physical parameters

$R(\text{m})$	$L/R$	$h_N/R$	$h_p/R$	$b/R$	$C_w(\text{N.S/m})$
$1 \times 10^{-9}$	10	0.01	0.005	0.1	$1 \times 10^{-3}$
$K_w(\text{N/m}^3)$	$K_p(\text{N/m})$	$V_p(\text{V})$	$V_0$	$V_{DC}(\text{V})$	$V_{AC}(\text{V})$
$8.999503 \times 10^{17}$	2.071273	$1 \times 10^{-2}$	1	2	1

### 3.1. Surface/interface effects on pull-in instability

In current section, the surface/interface parameters effect of piezoelectric nanosensor such as Lamé's constants ( $\lambda^{I,S}, \mu^{I,S}$ ), residual stress ( $\tau_0^{I,S}$ ), piezoelectric constants ( $e_{31p}^{S_k}, e_{32p}^{S_k}$ ) and mass density ( $\rho^{I,S}$ ) are studied for pull-in instability analysis on dimensionless natural frequency and nonlinear dynamics response in accordance with the data in Tables 1-3. First, the effect of direct pull in voltage DC as pull-in instability analysis on the DNF of PENS is presented in Fig. 2 and for different boundary conditions and two cases of surface/interface densities of Table 4. It is obvious from this Figure that in higher surface/interface densities of case 1, stiffness is decrease and the natural frequency decrease to without S/I effects. Also, with decreasing of surface/interface densities in case 2, stiffness increase and the natural frequency is increased compared to without S/I effects. Also, this figure shown that the lowest and highest natural frequency respectively are for case 2 of CC boundary condition and case 1 of CF boundary condition both with S/I effects. In all boundary conditions, case 2 (1) of Table 4 considering all S/I effects have maximum (minimum) pull in voltage and natural frequency.

**Table 4** Two cases of surface/interface densities

Case 1		Case 2	
$\rho^I(\text{kg/m}^2)$	$\rho^S(\text{kg/m}^2)$	$\rho^I(\text{kg/m}^2)$	$\rho^S(\text{kg/m}^2)$
$5.46 \times 10^{-7}$	$5.61 \times 10^{-6}$	$5.46 \times 10^{-8}$	$5.61 \times 10^{-7}$

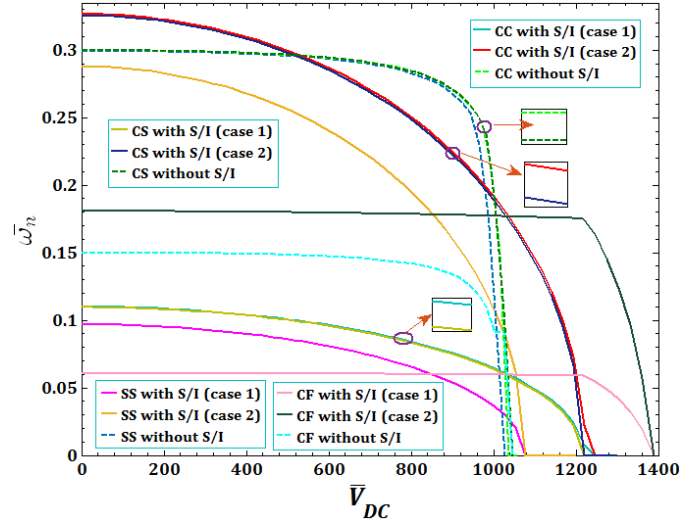


**Fig. 2** The effects of different boundary conditions for pull in voltage on DNF of PENS

Figs. 3 and 4 present the effects of different surface/ interface Lamé's constants  $\lambda^{S_k}$  and  $\lambda^{I_k}$ , for pull-in instability analysis respectively on DNF and NDR of PENS.

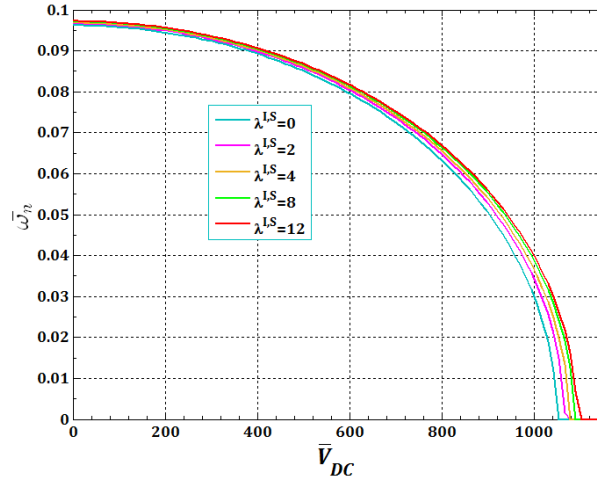


**Fig. 3** The effects of surface/interface Lamé's constants  $\lambda^{I,S}$  for pull in voltage on DNF of SS PENS

It is clear that increasing both surface/interface Lamé's constants  $\lambda^{I,S}$ , due to increasing of PENS stiffness, in both analysis of DNF and NDR, pull-in voltage increases. Also, it is obvious that for different cases of Lamé's constants, the system has stable (for example:  $A$  to  $B_1$  or  $C_1$  from Fig. 4) or unstable (for example:  $B_1$  to  $B_2$  or  $C_1$  to  $C_2$  from Fig. 4) point as saddle node bifurcation point.

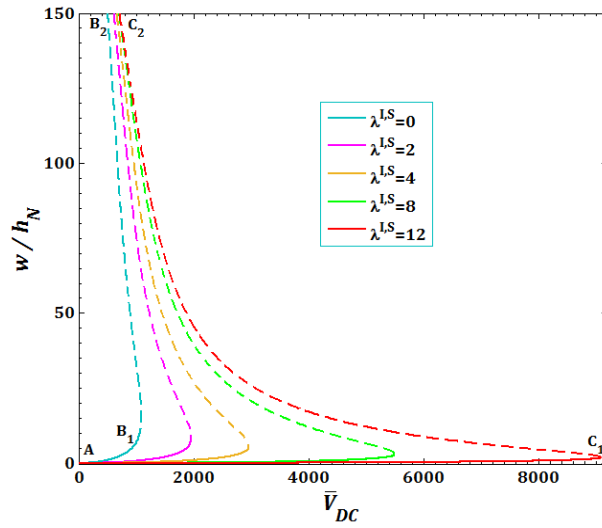


**Fig. 4** Influence of surface/interface Lamé's constants  $\lambda^{I,S}$  for pull in voltage on NDR of SS PENS with  $\bar{V}_p = 1 \times 10^{-3}$ ; solid line (-): stable, dashed line (--): unstable

The effects of different surface and interface Lamé's constants  $\mu^{S,k}$ , and  $\mu^{I,k}$ , for pull-in instability analysis respectively on DNF and NDR of PENS are presented in Figs. 5 and 6.

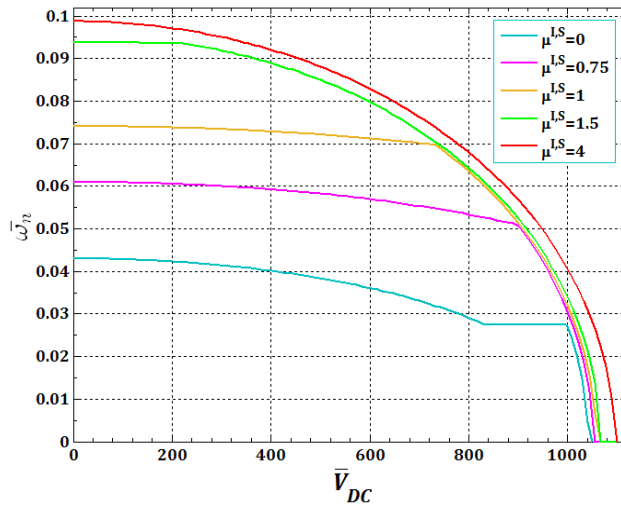


**Fig. 5** The effects of surface/interface Lamé's constants  $\mu^{I,S}$  for pull in voltage on DNF of SS PENS

Similar to  $\lambda^{I,S}$ , it is clear that increasing both surface/interface Lamé's constants  $\mu^{I,S}$ , due to increasing of PENS stiffness, in both analysis of DNF and NDR, pull-in voltage increases.

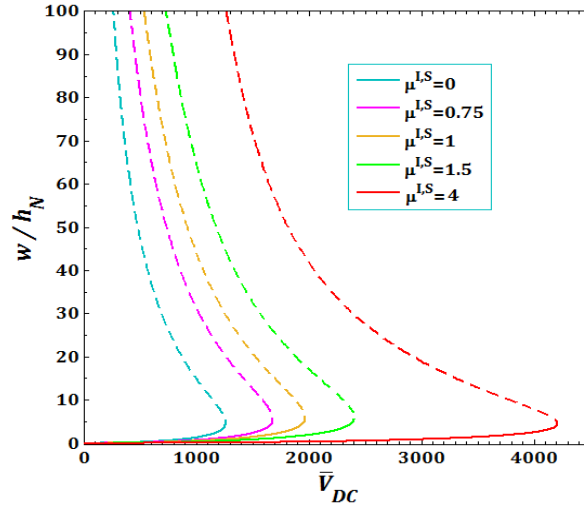


**Fig. 6** Influence of surface/interface Lamé's constants  $\mu^{I,S}$  for pull in voltage on NDR of SS PENS with  $\bar{V}_p = 1 \times 10^{-3}$ ; solid line (-): stable, dashed line (--): unstable

Figs. 7 and 8 show the effects of surface and interface residual stress  $\tau_0^{S,k}$  and  $\tau_0^{I,k}$ , for pull-in instability analysis respectively on DNF and NDR of PENS.

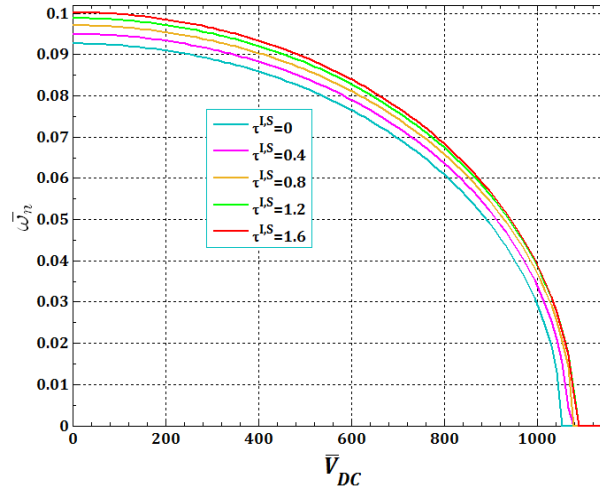


**Fig. 7** The effects of surface/interface residual stress  $\tau_0^{I,S}$  for pull in voltage on DNF of SS PENS

As can be show in both analysis of DNF and NDR, increasing both surface/interface residual stress  $\tau_0^{I,S}$  lead to increasing of PENS stiffness and as a result, pull-in voltage increases.



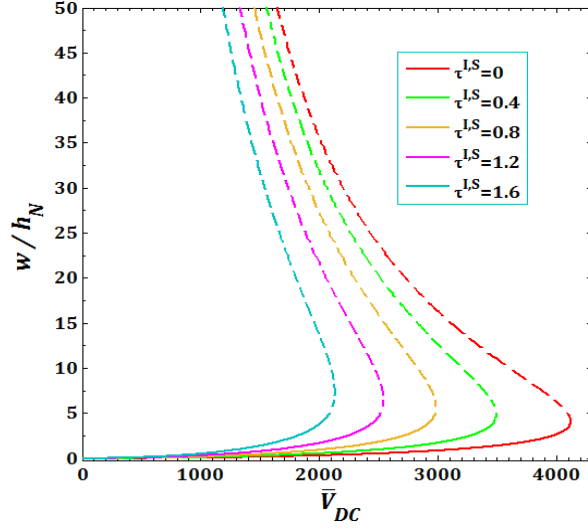


**Fig. 8** Influence of surface/interface residual stress  $\tau_0^{I,S}$  for pull in voltage on NDR of SS PENS with  $\bar{V}_p = 1 \times 10^{-3}$ ; solid line (-): stable, dashed line (--): unstable

The effect of surface piezoelectricity constants  $e_{31p}^{S_k}$  and  $e_{32p}^{S_k}$  for pull-in instability analysis respectively on DNF and NDR of PENS are presented in Figs. 9 and 10.

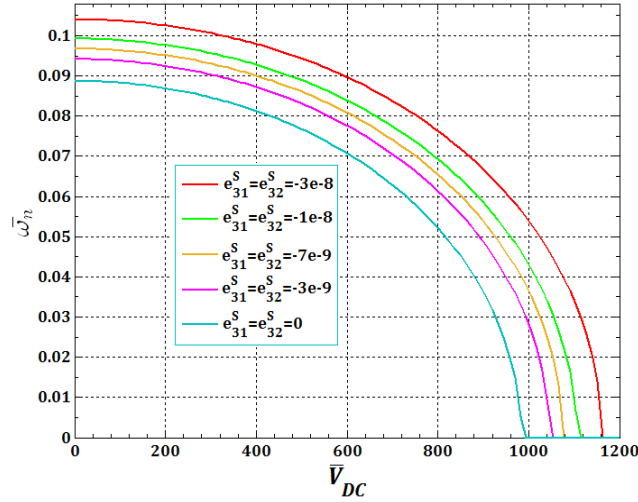


**Fig. 9** The effects of surface piezoelectricity constants  $e_{31p}^{S_k}, e_{32p}^{S_k}$  for pull in voltage on DNF of SS PENS

It is observed that increasing of negative surface piezoelectricity constants  $e_{31p}^{S_k}$  and  $e_{32p}^{S_k}$  leads to increasing of the PENS stiffness and as a result, pull-in voltage increases.

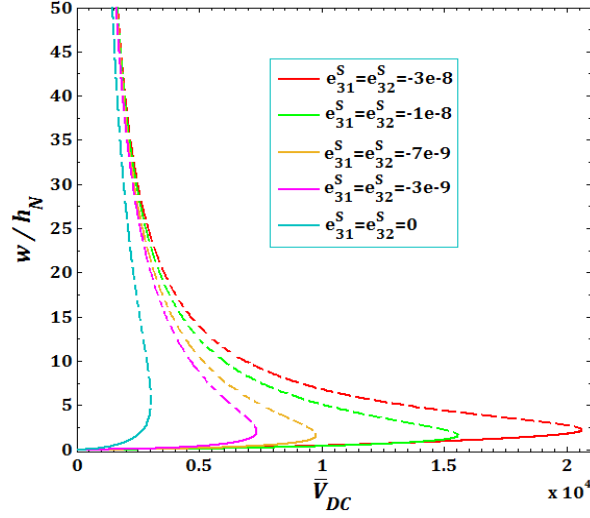


**Fig. 10** Influence of surface piezoelectricity constants  $e_{31p}^{Sk}, e_{32p}^{Sk}$  for pull in voltage on NDR of SS PENS with  $\bar{V}_p = 1 \times 10^{-3}$ ; solid line (-): stable, dashed line (--): unstable

Figs. 11 and 12 illustrate the effects of surface and interface mass density  $\rho^{Sk}$  and  $\rho^{Ik}$ , for pull-in instability analysis respectively on DNF and NDR of PENS. As it can be seen that with increasing surface/interface mass density  $\rho^{IS}$ , due to decreasing of the PENS stiffness, DNF significantly decrease, but will not have a considerable effect on pull-in voltage and NDR.

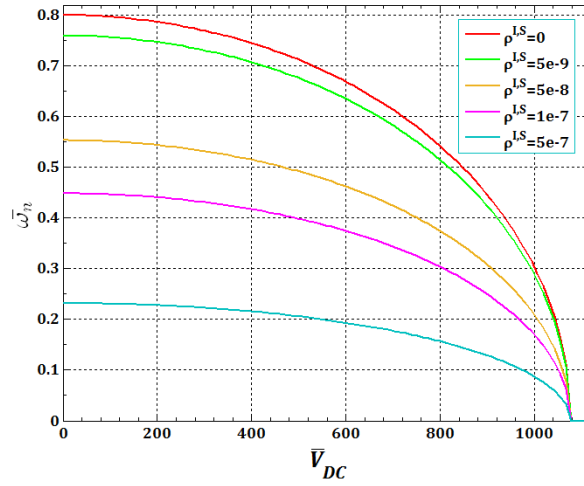


**Fig. 11** The effect of surface  $\rho^S$  and Interface  $\rho^I$  mass density for pull in voltage on DNF of SS PENS

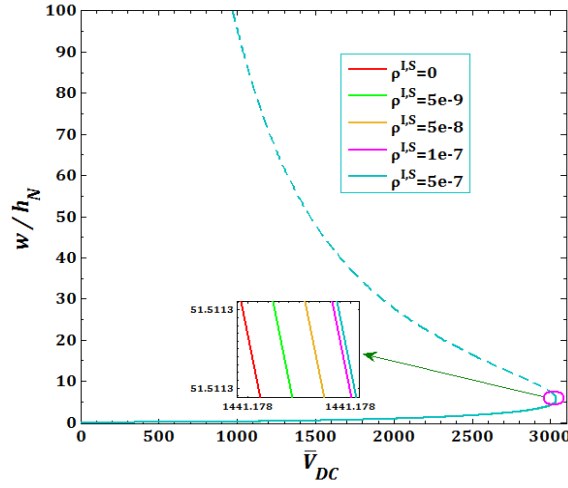


**Fig. 12** Influence of surface  $\rho^S$  and Interface  $\rho^I$  mass density for pull in voltage on NDR of SS PENS with  $\bar{V}_p = 1 \times 10^{-3}$ ; solid line (-): stable, dashed line(--): unstable

In Figs. 13 and 14 the effects of surface/interface parameters effects for pull-in instability analysis respectively on DNF and NDR of SS PENS are shown. It can be seen that with ignoring the surface/interface density  $\rho^{l,S}$ , due to increasing of PENS stiffness, the system will have a maximum DNF compared to other cases. Also considering the surface/interface effects of case 1 in Table 4, due to decreasing of nano shell stiffness, has a lower DNF than the case of without S/I effects. According to this Figure, regardless the Lamé's constants  $\lambda^{l,S}$  and S/I stress ( $\tau_0^{l,S}$ ) slightly lead to decreasing of PENS stiffness and as a result, the DNF is lower than the case of with all S/I effects. The surface piezoelectric constants ( $e_{31p}^{S_k}, e_{32p}^{S_k}$ ) do not have much effect on the DNF.

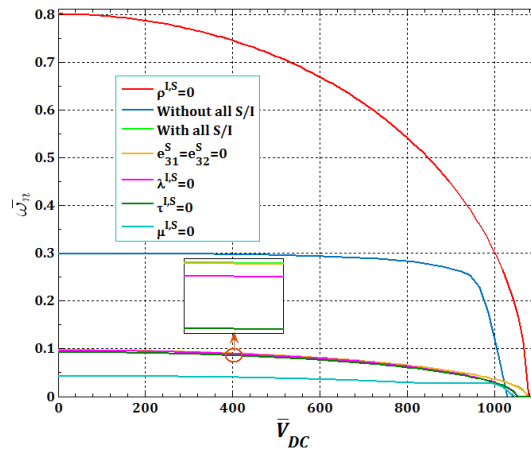


**Fig. 13** The effects of all surface and interface parameters for pull in voltage on DNF of SS PENS

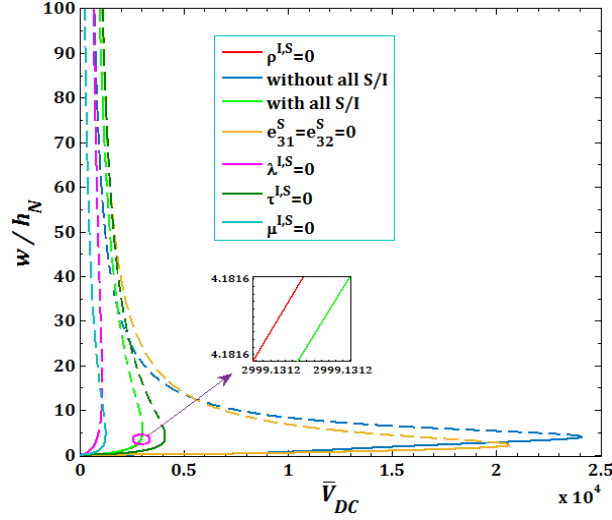


**Fig. 14** Influence of surface/interface Lamé's constants  $\lambda^{I,S}$  for pull in voltage on NDR of SS PENS with  $\bar{V}_p = 1 \times 10^{-3}$ ; solid line (-): stable, dashed line (--): unstable

Also, it can be seen that in DNF analysis, ignoring the surface/interface density  $\rho^{I,S}$ , surface piezoelectric constants ( $e_{31p}^{S_k}, e_{32p}^{S_k}$ ) and with all S/I, the SS PENS has maximum pull-in voltage, while in NDR analysis of SS PENS, in case of without all S/I has maximum pull-in voltage.

#### 4. CONCLUSION

In current study, the effect of surface/interface parameters of piezoelectric nanosensor such as Lamé's constants ( $\lambda^{I,S}, \mu^{I,S}$ ), residual stress ( $\tau_0^{I,S}$ ), piezoelectric constants ( $e_{31p}^{S_k}, e_{32p}^{S_k}$ ) and mass density ( $\rho^{I,S}$ ) are studied for pull-in instability analysis on dimensionless natural frequency and nonlinear dynamics response. The piezoelectric nanosensor is subjected to two piezoelectric layers, nonlinear electrostatic force, harmonic excitations and structural damping. To achieve this purpose, the Hamilton's approach, assumed mode and Lagrange–Euler's theories and also arc-length continuation and complex averaging methods are used. Some conclusions are obtained from this study:

- In the case of lower (higher) surface/interface densities, its stiffness is increase (reduced) that leads to increasing (decreasing) of the natural frequency compared to case of without S/I effects.
- The CF (CC) boundary condition with S/I case1 (2) has the lowest (highest) natural frequency.
- Increasing surface/interface Lamé's constants  $\lambda^{I,S}$  and  $\mu^{I,S}$ , surface/interface residual stress  $\tau_0^{I,S}$  and negative surface piezoelectricity constants  $e_{31p}^{S_k}$  and  $e_{32p}^{S_k}$ , due to increasing of PENS stiffness, in both analysis of DNF and NDR lead to increasing of pull-in voltage.

- With increasing surface/interface mass density  $\rho^{L,S}$ , due to decreasing of the PENS stiffness, DNF significantly decrease, but will not have a significant impact on pull-in voltage and NDR.
- In DNF analysis, ignoring the surface/interface density  $\rho^{L,S}$ , surface piezoelectric constants ( $e_{31p}^{S_k}, e_{32p}^{S_k}$ ) and with all S/I, the SS PENS has maximum pull-in voltage, while in NDR analysis of SS PENS, in case of without all S/I has maximum pull-in voltage.
- For different surface/interface parameters in NDR analysis, the system has stable or unstable point with saddle-node bifurcation point.

## REFERENCES

1. Tzou, H., 2019, *Piezoelectric Shells: Sensing, Energy Harvesting, and Distributed Control*, Springer, USA.
2. Wang, L., Chen, W., Liu, J., Deng, J., Liu, Y., 2011, *A review of recent studies on non-resonant piezoelectric actuators*, Mechanical Systems and Signal Processing, 11(4), pp. 187-96.
3. Nayfeh, A.H., Ouakad, H.M., Najjar, F., Choura, S., Abdel-Rahman, E.M., 2010, *Nonlinear dynamics of a resonant gas sensor*, Nonlinear Dynamics, 59, pp. 607–618.
4. Farokhi, H., Païdoussis, M. P., Misra, A., 2018, *Nonlinear behaviour of cantilevered carbon nanotube resonators based on a new nonlinear electrostatic load model*, Journal of Sound and Vibration, 49, pp. 604-629.
5. Prasanth, C.S.R., Harsha, C.S., Pratiher, B., 2018, *Electrostatic pull-in analysis of a nonuniform micro-resonator undergoing large elastic deflection*, Proceedings of the Institution of Mechanical Engineers, Part C: Journal of Mechanical Engineering Science, 18(232), pp. 3337-3350.
6. Pourkiaee, S. M., Khadem, S. E., Shahgholi, M., Bab, S., 2017, *Nonlinear modal interactions and bifurcations of a piezoelectric nanoresonator with three-to-one internal resonances incorporating surface effects and van der Waals dissipation forces*, Nonlinear Dynamics, 88, pp. 1785–1816.
7. Karimipour, I., Tadi Beni, Y., Zeighampour, H., 2018, *Nonlinear size-dependent pull-in instability and stress analysis of thin plate actuator based on enhanced continuum theories including nonlinear effects and surface energy*, Microsystem Technologies, 24, pp. 1811–1839.
8. Nikpourian, A. R., Ghazavi, M. R., Azizi, S., 2018, *On the nonlinear dynamics of a piezoelectrically tuned micro-resonator based on non-classical elasticity theories*, International Journal of Mechanics and Materials in Design, 14, pp. 1–19.
9. Zhang, W.M., Yan, H., Peng, Z.K., Meng, G., 2014, *Electrostatic pull-in instability in MEMS/NEMS: A review*, Sensors and Actuators A: Physical, 214, pp. 187–218.
10. Sedighi, H.M., 2014, *Size-dependent dynamic pull-in instability of vibrating electrically actuated microbeams based on the strain gradient elasticity theory*, Acta Astronautica, 95, pp. 111-123.
11. Sedighi, H.M., Koochi, A., Daneshmand, F., Abadyan, M., 2015, *Non-linear dynamic instability of a double-sided nano-bridge considering centrifugal force and rarefied gas flow*, International Journal of Non-Linear Mechanics, 77, pp. 96-106.
12. Y. Tadi Beni, I. Karimipour, M. Abadyan, 2014, *Modeling the instability of electrostatic nano-bridges and nano-cantilevers using modified strain gradient theory*. Applied Mathematical Modelling. 39, 2633-2648.
13. Tadi Beni, Y., Karimipour, I., Abadyan, M., 2014, *Modeling the effect of intermolecular force on the size-dependent pull-in behavior of beam-type NEMS using modified couple stress theory*, Journal of Mechanical Science and Technology, 28, pp. 3749-3757.
14. Tadi Beni, Y., 2016, *Size-dependent analysis of piezoelectric nanobeams including electro-mechanical coupling*, Mechanics Research Communications, 75, pp. 67–80.
15. Tajalli, S. A., Tajalli, S. M., 2019, *Wavelet based damage identification and dynamic pull-in instability analysis of electrostatically actuated coupled domain microsystems using generalized differential quadrature method*, Mechanical Systems and Signal Processing, 133, 106256.
16. Farokhi, H., Misra, A. K., Païdoussis, M. P., 2017, *A new electrostatic load model for initially curved carbon nanotube resonators: pull-in characteristics and nonlinear resonant behaviour*, Nonlinear Dynamics, 88, pp. 1187–1211.
17. Amabili, M., 2008, *Nonlinear Vibrations and Stability of Shells and Plates*, Cambridge University Press, New York.

18. Bornassi, S., Haddadpour, H., 2017, *Nonlocal vibration and pull-in instability analysis of electrostatic carbon-nanotube based NEMS devices*, Sensors and Actuators A: Physical, 266, pp. 185-196.
19. Gurtin, M.E., Murdoch, A.I., 1975, *A continuum theory of elastic material surface*, Archive for Rational Mechanics and Analysis, 57, pp. 291-323.
20. Gurtin, M.E., Murdoch, A.I., 1978, *Surface stress in solids*, International Journal of Solids and Structures, 14, pp. 431-40.
21. Fang, X.Q., Zhu, C.S., Liu, J.X., Liu, X.L., 2018, *Surface energy effect on free vibration of nano-sized piezoelectric double-shell structures*, Physica B: Condensed Matter, 529, pp. 41-56.
22. Fang, X.Q., Zhu, C.S., Liu, J.X., Zhao, J., 2018, *Surface energy effect on nonlinear buckling and postbuckling behavior of functionally graded piezoelectric cylindrical nanoshells under lateral pressure*, Materials Research Express, 5.4, 045017.
23. Hashemi Kachapi, Sayyid H., Dardel, M., Mohamadi daniali, H., Fathi, A., 2019, *Effects of surface energy on vibration characteristics of double-walled piezo-viscoelastic cylindrical nanoshell*, Proceedings of the Institution of Mechanical Engineers, Part C: Journal of Mechanical Engineering Science, 15(233), pp. 5264-5279.
24. Hashemi Kachapi, Sayyid H., Dardel, M., Mohamadi daniali, H., Fathi, A., 2019, *Pull-in instability and nonlinear vibration analysis of electrostatically piezoelectric nanoresonator with surface/interface effects*, Thin-Walled Structures, 143, 106210.
25. Hashemi Kachapi, Sayyid H., Dardel, M., Mohamadi daniali, H., Fathi, A., 2019, *Nonlinear dynamics and stability analysis of piezo-visco medium nanoshell resonator with electrostatic and harmonic actuation*, Applied Mathematical Modelling, 75, pp. 279-309.
26. Hashemi Kachapi, Sayyid H., Dardel, M., Mohamadi daniali, H., Fathi, A., 2019, *Nonlinear vibration and stability analysis of double-walled piezoelectric nanoresonator with nonlinear van der Waals and electrostatic excitation*, Journal of Vibration and Control, 9-10(26), pp. 680-700.
27. Hashemi Kachapi, Sayyid H., Mohamadi daniali, H., Dardel, M., Fathi, A., 2020, *The effects of nonlocal and surface/interface parameters on nonlinear vibrations of piezoelectric nanoresonator*, Journal of Intelligent Material Systems and Structures, 31(6), pp. 818-842.
28. Hashemi Kachapi, Sayyid H., 2020, *Nonlinear and nonclassical vibration analysis of double walled piezoelectric nano-structure*, Advances in Nano Research, An International Journal, 9(4).
29. Fan, T., 2015, *Nano-scale energy harvester of piezoelectric/piezomagnetic structures with torsional mode*, Mechanical Systems and Signal Processing, 26, pp. 1150-1163.
30. Manevitch, A.I., Manevitch, L.I., 2005, *The mechanics of Nonlinear Systems with Internal Resonance*, Imperial College Press, London.